

An Operational Definition of Topological Order

Amit Jamadagni* and Hendrik Weimer

Institut für Theoretische Physik, Leibniz Universität Hannover, Appelstraße 2, 30167 Hannover, Germany

The unrivaled robustness of topologically ordered states of matter against perturbations has immediate applications in quantum computing and quantum metrology, yet their very existence poses a challenge to our understanding of phase transitions. However, a comprehensive understanding of what actually constitutes topological order is still lacking. Here we show that one can interpret topological order as the ability of a system to perform topological error correction. We find that this operational approach corresponding to a measurable both lays the conceptual foundations for previous classifications of topological order and also leads to a successful classification in the hitherto inaccessible case of topological order in open quantum systems. We demonstrate the existence of topological order in open systems and their phase transitions to topologically trivial states. Our results demonstrate the viability of topological order in nonequilibrium quantum systems and thus substantially broaden the scope of possible technological applications.

INTRODUCTION

Topologically ordered phases are states of matter that fall outside of Landau's spontaneous symmetry breaking paradigm and cannot be characterized in terms of local order parameters, as it is the case with conventional symmetry-breaking phase transitions. From a broad perspective, they can be classified into symmetry-protected topological order or intrinsic topological order [1]. For the former, the existence of a symmetry is required to maintain topological order, i.e., when the symmetry is broken the system immediately returns to a topologically trivial state. In some cases, topological order can be captured in terms of topological invariants such as the Chern number [2, 3], but being based on single-particle wave functions, their extension to interacting systems is inherently difficult [4]. Alternatively, topological order has been discussed in terms of nonlocal order parameters often related to string order [5–8], but the main difficulty of this approach is that such string order can also be observed in topologically trivial phases [9]. From a conceptual point of view, a particularly attractive definition of topological order is the impossibility to create a certain quantum state from a product state by a quantum circuit of finite depth [10]. However, since this is equivalent to the uncomputable quantum Kolmogorov complexity [11], it has very little practical applications. Hence, most analyses of topological ordered systems have been centered around indirect signatures such as the topological entanglement entropy [12–14] or minimally entangled states [15, 16], but even those quantities can prove difficult to interpret [17, 18].

Here, we overcome the limitations of the previous approaches to topological order by understanding topological order as the intrinsic ability of a system to perform topological error correction, giving rise to an operational definition of topological order that can be readily computed. Our definition is thus connected to taking the robustness of topological phases as its defining property [19, 20], see the Supplementary Methods for a detailed

technical discussion. To make our definition mathematically precise, we call a system to be in a topologically ordered state if it can be successfully corrected by an error correction circuit of finite depth. One key advantage of our approach is that the error correction circuit does not have to be optimal, as it only requires to reproduce the correct finite size scaling properties, which can be expected to be universal across a topological phase transition. This puts our approach in stark contrast with the classification of topological error correction codes in terms of their threshold values [21], as the latter is a nonuniversal quantity. Symmetry protected topological order can be represented within our error correction formalism by imposing certain symmetry constraints on the error correction circuit. Compared to previous approaches to topological order, another striking advantage of our error correction method is that it corresponds to an actual observable, which can be measured in an experiment.

RESULTS

Operational definition for closed systems

To demonstrate the viability of our error correction approach in a concrete setting, we turn to the toric code model, which serves as a paradigm for intrinsic topological order [22]. Its Hamiltonian is given by a sum over two classes of spin 1/2 operators describing four-body interactions, A_v and B_p , acting on vertices v and plaquettes p , respectively, according to

$$H_{TC} = -E_0 \left(\sum_v \underbrace{\sigma_\alpha^x \sigma_\beta^x \sigma_\gamma^x \sigma_\delta^x}_{A_v} + \sum_p \underbrace{\sigma_\mu^z \sigma_\nu^z \sigma_\rho^z \sigma_\sigma^z}_{B_p} \right), \quad (1)$$

where $\sigma_i^{x,z}$ denotes the Pauli matrix acting on site i . The robustness of topological order of the ground state can be analyzed with respect to the response of a perturbation

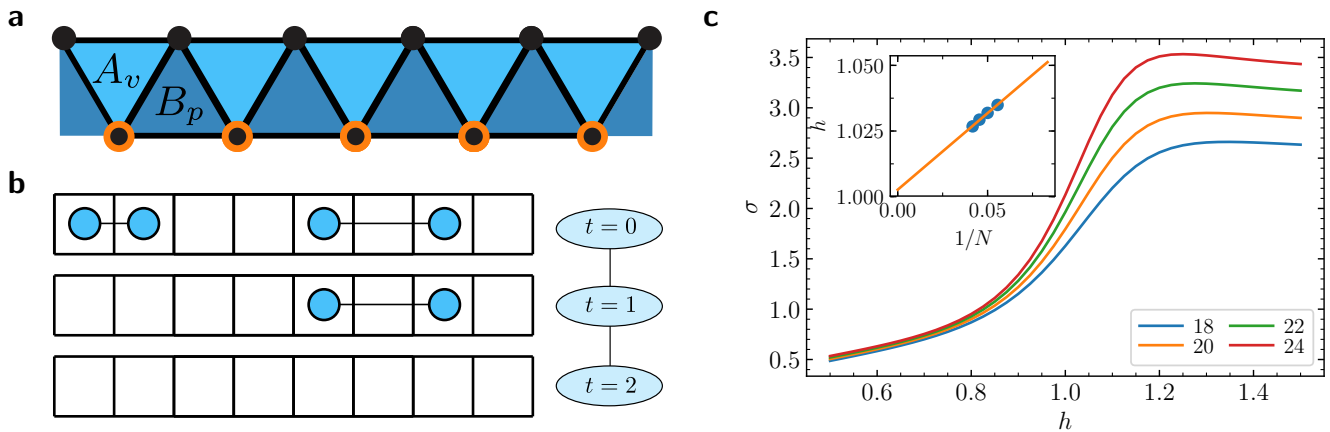


FIG. 1. Topological order in a quasi-1D toric code model. (a) The A_v and B_p operators are arranged along two rails of sites such that the perturbation on the lower rail (orange) maps onto the 1D transverse field Ising model. (b) Example of the error correction procedure for $N = 8$ Ising spins containing four errors, with the state of the system shown after t timesteps of the algorithm. The errors are fused along the horizontal strings, with the total error correction depth being $t_d = 2$. (c) Standard deviation n_σ of the circuit depth for different system sizes. Above the topological transition, the circuit depth diverges in the thermodynamic limit, with a finite size scaling analysis (inset) yielding critical value of $h_c = 1.003(1)$.

describing a magnetic field, i.e., $H = H_{TC} - h \sum_i \sigma_i^x$. Importantly, the perturbed toric code can be mapped onto an Ising model in a transverse field using a highly non-local unitary transformation [23]. The phase transition from the topologically ordered to the trivial state then corresponds to the phase transition between the paramagnet and the ferromagnet in the Ising model [24]. Here, we will be interested in the case where the perturbed toric code can be mapped exactly onto the one-dimensional (1D) Ising model, which can be realized by imposing the right boundary condition [18], see Fig. 1. Our approach has the advantage that the critical point of the topological phase transitions is known to be exactly at $h_c = 1$. As there is no intrinsic topological order in 1D systems, the phase for $h < 1$ is actually a symmetry-protected topological phase, with the protected symmetry being the Z_2 symmetry of the associated Ising model. Additionally, note that the quasi-1D nature of the toric code model results in the four-body interactions in Eq. (1) being replaced by three-body interactions.

For the topological order arising in the toric code, the required topological error correction can be readily expressed in terms of the Ising variables $S_v = A_v$ and $S_p = B_p$, where each spin having $S_i^z = -1$ corresponds to the presence of an error. As a first step of the error correction algorithm, a syndrome measurement is performed, i.e., all the Ising spins are measured in their S^z basis, corresponding to the measurement of both the A_v and B_p degrees of freedom in the original toric code model. Under the perturbation, the observables S_i^z exhibit quantum fluctuations, therefore it is necessary to perform a statistical interpretation of the depth of the error correction circuit. Here, we find that the standard deviation of the circuit depth exhibits substantially better finite

size scaling behavior than the mean, hence we use the former for the detection of topological order in the following. The error correction circuit is then implemented in a massively parallel way by decorating each of the detected errors by a walker that travels through the system until it encounters another error, upon which the two errors are fused and removed from the system [25], see the Methods section for details. Figure 1 demonstrates that our error correction approach is indeed able to detect the topological phase transition, including the identification of the correct critical point at $h_c = 1$. Crucially, we want to stress that our notion of error correction is not limited to toric code models. In the Supplementary Discussion, we consider the cubic code model [26] hosting fracton topological order [27].

Topological order in open quantum systems

Let us now extend our approach to mixed quantum states, where previous works have shed some light on topological properties [28–33], but a universally applicable definition of topological order has remained elusive so far. This extension is straightforward, as the implementation of the topological error correction channel can be applied to mixed states as well. Here, we consider mixed states arising in open quantum systems with purely dissipative dynamics given in terms of jump operators c_i according to the Markovian quantum master equation $d\rho/dt = \sum_i c_i \rho c_i^\dagger - \{c_i^\dagger c_i, \rho\}/2$. Dissipative variants of the toric code can be constructed by considering the jump

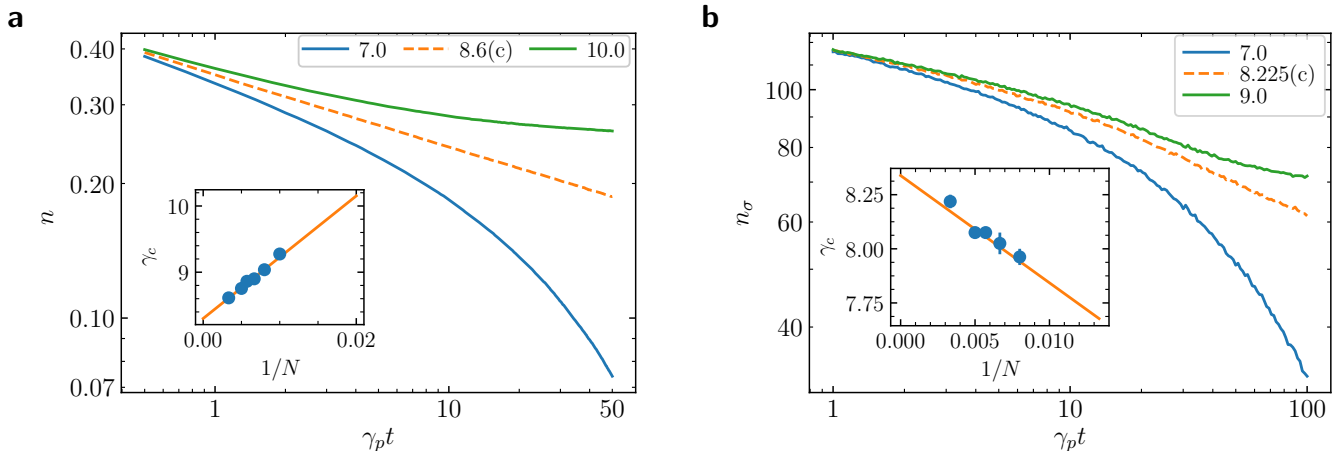


FIG. 2. Topological absorbing state transition. Error density n_e (a) and circuit depth n_σ (b) for $N = 300$ sites and different values of γ , showing subcritical behavior (blue), critical behavior (orange), and supercritical behavior (green). Initial states were chosen to have maximum n_e or n_σ , respectively. Finite size scaling leads to $\gamma_c = 8.30(2)$ (a, inset) and $\gamma_c = 8.34(5)$ (b, inset) in the thermodynamic limit.

operators

$$c_i^v = \sqrt{\gamma_v} \sigma_i^z (1 - A_v) / 2, i \in v \quad (2)$$

$$c_i^p = \sqrt{\gamma_p} \sigma_j^x (1 - B_p) / 2, j \in p \quad (3)$$

with rates $\gamma_{v,p}$, which result in the toric code ground states being steady states of the quantum master equation [34]. As before, we now consider the robustness of topological order to an additional perturbation. Here, we will first consider again a quasi one-dimensional model analogous to Fig. 1a, in which the perturbation is given by

$$c_i^h = \sqrt{\gamma} \sigma_i^x (1 - B_p) / 2, i \in p + 1,$$

with i being restricted to the upper rail. Note that in contrast to the jump operator of Eq. (2), this jump operator involves a spin that is part of the plaquette $p + 1$ and not of the plaquette p . This multi-plaquette operator leads to a heating process introducing new errors, while the jump operators of Eqs. (2, 3) describe cooling processes that remove errors from the system. Importantly, the creation of a new error on the plaquette $p + 1$ requires the existence of another error on the neighboring plaquette p , which is also reflected after mapping onto Ising variables, see the Methods section for details. This results in the model falling into the well-known class of absorbing state models [35], with the toric code ground state corresponding to the absorbing state. Such absorbing state models can exhibit phase transitions to an active phase where the absorbing state is no longer reached asymptotically when starting from a different initial state. Here, we indeed find such a phase transition in the density of errors, see Fig. 2. Moreover, this absorbing-to-active transition is also accompanied by a divergence of the depth of the error correction circuit, i.e., by a topological transition

to a trivial phase. We also track the critical exponent δ measuring the algebraic decay of the density of errors n_e or the circuit depth n_σ , respectively, by considering the quantity

$$\delta_{\text{eff}}(t) = -\frac{1}{\log m} \log \frac{n_{e,\sigma}(mt)}{n_{e,\sigma}(t)} \quad (4)$$

which remains constant for a fixed value of m [35]. In the limit of large system sizes, both the critical strength for the transition and the critical exponent are in close agreement between the absorbing-to-active transition and the topological transition, see Fig. 3, belonging to the universality class of one-dimensional directed percolation ($\delta = 0.163$ [35]).

Importantly, our approach to topological order can also be readily applied to higher-dimensional systems. Here, we will be interested in a two-dimensional absorbing state model, in which both error types are present. In particular, the creation of A_v errors is conditional on the existence of a neighboring B_p error and vice versa. Hence, we consider jump operators of the form

$$c_i^{hv} = \sqrt{\gamma} \sigma_i^x (1 - A_v) / 2$$

$$c_i^{hp} = \sqrt{\gamma} \sigma_i^z (1 - B_p) / 2.$$

Importantly, the lack of boundary processes now leads to a conservation of the parity of both type of errors. This model can be expected to be in the same universality class as two-dimensional branching-annihilating random walks with two species [36]. While the model is active for any finite γ , it exhibits nontrivial critical behavior, having an exponent $\delta = 1$ with logarithmic corrections. Figure 4 shows the data collapse for different system sizes for both the error density and the circuit depth, confirming this picture. Strikingly, the logarithmic corrections in

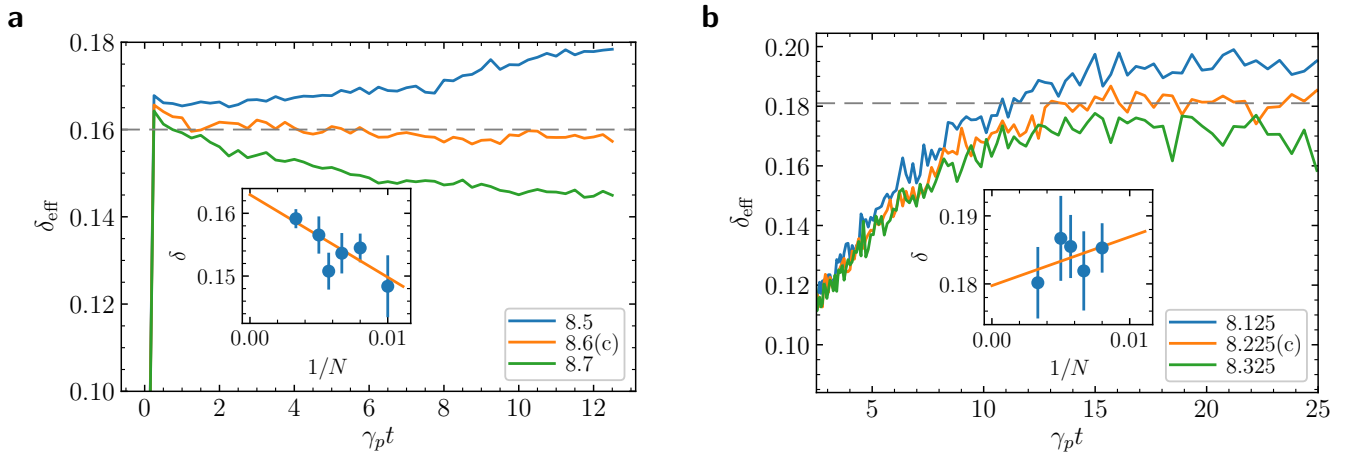


FIG. 3. Effective critical exponents according to Eq. (4) for the absorbing-active transition (a) and the topological transition (b) ($m = 4$). The critical value of the transition is taken where δ_{eff} remains constant. Error bars correspond to all values consistent with a constant value in the long time limit. Finite size scaling leads to $\delta = 0.163(5)$ (a, inset) and $\delta = 0.18(2)$ (b, inset) in the thermodynamic limit. Errors are given by the sum of the uncertainty in the linear fit and the difference in δ between $m = 4$ and $m = 2$.

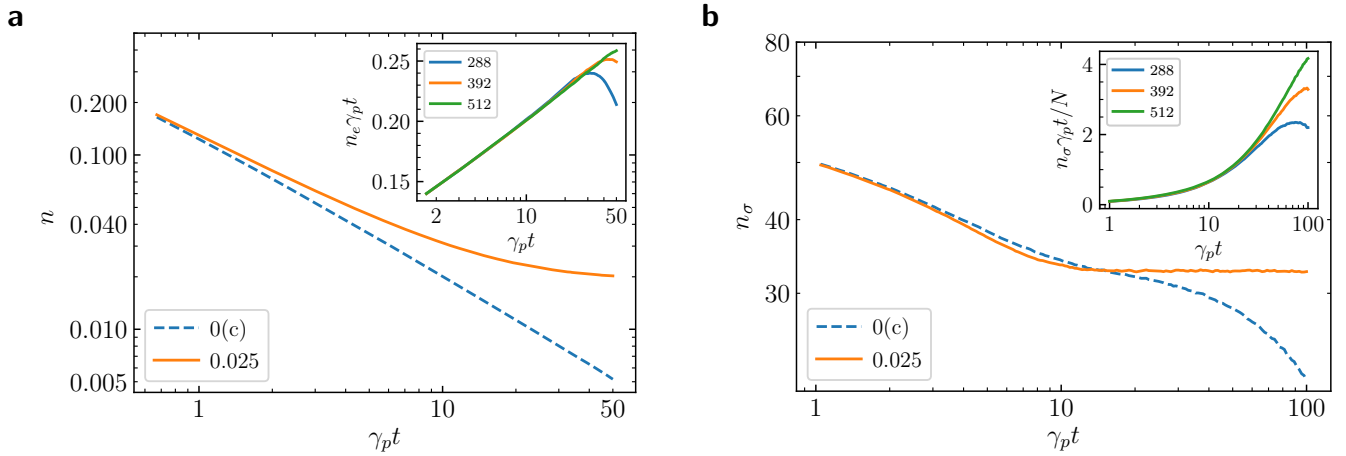


FIG. 4. Two-dimensional topological criticality. Error density n_e (a) and circuit depth n_σ (b) for $N = 512$ sites and $\gamma = 0$ (dashed) and $\gamma = 0.025 \gamma_p$ ($\gamma_p = \gamma_v$). The insets show the logarithmic corrections to a t^{-1} decay, with a linear behavior for the error density (a) and a quadratic behavior for the topological transition (b) before finite size effects become relevant.

the topological case include a quadratic term that is not present in the error density, pointing to a different critical behavior. This demonstrates that topological criticality cannot be predicted using only the properties of an accompanying conventional phase transition.

Summary

In summary, we have introduced a novel operational approach to topological order based on the ability to perform topological error correction. Our method reproduces known topological phase transitions and can be readily applied to previously inaccessible cases such as

topological transitions in open quantum systems, and has the additional advantage that it corresponds to a measurable observable. Furthermore, we would like to note that our approach can be readily applied to other topologically ordered systems. For instance, both the Kitaev wire [37] and Haldane insulators [38] can be mapped onto effective spin models, where an analogous error correction strategy can be performed. Finally, our work paves the way for many future theoretical and experimental investigations, such as the application of our approach to fracton [26, 27, 39] or Floquet [40, 41] topological order, or the direct experimental realization of the error correction protocol presented in our work for the development of future quantum technological devices.

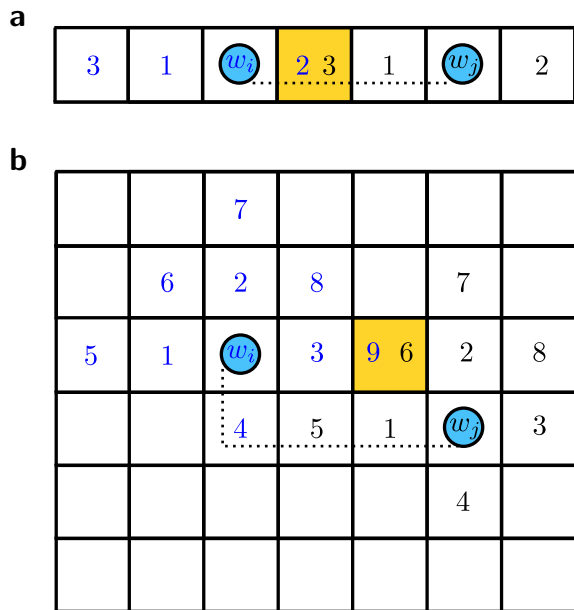


FIG. 5. Schematic representation of the error correction procedure. Two errors are associated with walkers w_i (blue) and w_j (black), located at the errors at $t = 0$. The colored numbers indicate the timestep at which a particular walker visits a site. Once a walker encounters a site already visited by the other walker (yellow), the two errors can be fused along the dotted path. In one dimension (a), the walkers alternate in a left-right pattern, in two dimensions (b), the walkers proceed in diamond-shaped patterns corresponding to a constant Manhattan distance from the initial sites.

METHODS

Error correction in toric code models

The error correction scheme for the detection of topological order is based on the results from the error syndrome measurements, which can be cast in terms of the spin variables S_v and S_p . In cases where there are both error types being present, the error correction can be realized independently. As the figure of merit, we are interested in the depth of the classical error correction circuit, which maps the initial erroneous state onto the topologically ordered state without any errors. Our error correction procedure is massively parallelized, i.e., within a topologically ordered phase, it is able to remove a thermodynamically large number of errors in constant time. This is in stark contrast to the conventional maximum-likelihood error correction [42], as this will always require an error correction circuit whose depth scales with the system size. The same argument also holds for assessing topological order based on circuit complexity [43], as the circuit complexity is an extensive quantity even in the topologically ordered phase.

For each error, we decorate the associated site with

a walker w_i , which continuously explores the surroundings of the original site, looking for the presence of other errors. In one spatial dimension, the walker alternates between investigating sites on the left and on the right, while in two dimensions, this is generalized to continuously exploring sites with an increasing Manhattan distance to the original site, see Fig. 5. For simplicity, we assume that changing the site of a walker takes exactly one unit of time, irrespectively of the distance traveled. Once a walker encounters a site with either an error or a site previously visited by a walker w_j originating from another error, the error correction procedure starts. For this, the errors on site i and j are fused together along the shortest path, removing them and their associated walkers from the system. Here, we assume that the fusion is instantaneous, which does not modify the overall finite size scaling properties of the error correction circuit. The error correction procedure is performed until all errors have been removed from the system. In the one-dimensional case, we also allow for errors being removed via the left or right boundary of the system, preventing the case of a single error remaining without a potential fusion partner.

Ising-mapped jump operators

After mapping the system onto Ising variables S_i , we obtain a purely classical master equation, despite the basis states being highly entangled. Here, we take the limit $\gamma_v \rightarrow \infty$ such that the dynamics is restricted to the Ising spins related to the B_p operators. In the basis of the Ising spins S_i , we obtain the jump operators

$$c_i^p = \sqrt{\gamma_p} S_i^x S_{i+1}^x (1 - S_i^z) / 2$$

$$c_i^h = \sqrt{\gamma} S_{i+1}^x (1 - S_i^z) / 2.$$

DATA AVAILABILITY

The data that support the plots within this paper and other findings of this study are available from the corresponding author upon reasonable request.

CODE AVAILABILITY

All numerical codes in this paper are available upon request to the authors.

ACKNOWLEDGMENTS

We thank S. Diehl and T. Osborne for fruitful discussions. This work was funded by the Volkswagen Foundation, by the Deutsche Forschungsgemeinschaft (DFG,

German Research Foundation) within SFB 1227 (DQ-mat, project A04), SPP 1929 (GiRyd), and under Germany's Excellence Strategy – EXC-2123 QuantumFrontiers – 390837967.

AUTHOR CONTRIBUTIONS

Both authors contributed extensively to all parts of the manuscript.

COMPETING INTERESTS

The authors declare no competing interests.

* amit.jamadagni@itp.uni-hannover.de

- [1] Wen, X.-G. Colloquium: Zoo of quantum-topological phases of matter. *Rev. Mod. Phys.* **89**, 041004 (2017).
- [2] Thouless, D. J., Kohmoto, M., Nightingale, M. P. & den Nijs, M. Quantized Hall Conductance in a Two-Dimensional Periodic Potential. *Phys. Rev. Lett.* **49**, 405–408 (1982).
- [3] Kohmoto, M. Topological invariant and the quantization of the Hall conductance. *Ann. Phys. (N. Y.)* **160**, 343 – 354 (1985).
- [4] Fidkowski, L. & Kitaev, A. Effects of interactions on the topological classification of free fermion systems. *Phys. Rev. B* **81**, 134509 (2010).
- [5] den Nijs, M. & Rommelse, K. Preroughening transitions in crystal surfaces and valence-bond phases in quantum spin chains. *Phys. Rev. B* **40**, 4709–4734 (1989).
- [6] Haegeman, J., Pérez-García, D., Cirac, I. & Schuch, N. Order Parameter for Symmetry-Protected Phases in One Dimension. *Phys. Rev. Lett.* **109**, 050402 (2012).
- [7] Pollmann, F. & Turner, A. M. Detection of symmetry-protected topological phases in one dimension. *Phys. Rev. B* **86**, 125441 (2012).
- [8] Elben, A. *et al.* Many-body topological invariants from randomized measurements in synthetic quantum matter. *Science Adv.* **6** (2020).
- [9] Dalla Torre, E. G., Berg, E. & Altman, E. Hidden Order in 1D Bose Insulators. *Phys. Rev. Lett.* **97**, 260401 (2006).
- [10] Chen, X., Gu, Z.-C. & Wen, X.-G. Local unitary transformation, long-range quantum entanglement, wave function renormalization, and topological order. *Phys. Rev. B* **82**, 155138 (2010).
- [11] Mora, C. E., Briegel, H. J. & Kraus, B. Quantum Kolmogorov complexity and its applications. *Int. J. Quant. Inf.* **05**, 729–750 (2007).
- [12] Kitaev, A. & Preskill, J. Topological Entanglement Entropy. *Phys. Rev. Lett.* **96**, 110404 (2006).
- [13] Levin, M. & Wen, X.-G. Detecting Topological Order in a Ground State Wave Function. *Phys. Rev. Lett.* **96**, 110405 (2006).
- [14] Jiang, H.-C., Wang, Z. & Balents, L. Identifying topological order by entanglement entropy. *Nature Phys.* **8**, 902–905 (2012).
- [15] Zhang, Y., Grover, T., Turner, A., Oshikawa, M. & Vishwanath, A. Quasiparticle statistics and braiding from ground-state entanglement. *Phys. Rev. B* **85**, 235151 (2012).
- [16] Zhu, W., Sheng, D. N. & Haldane, F. D. M. Minimal entangled states and modular matrix for fractional quantum Hall effect in topological flat bands. *Phys. Rev. B* **88**, 035122 (2013).
- [17] Bridgeman, J. C., Flammia, S. T. & Poulin, D. Detecting topological order with ribbon operators. *Phys. Rev. B* **94**, 205123 (2016).
- [18] Jamadagni, A., Weimer, H. & Bhattacharyya, A. Robustness of topological order in the toric code with open boundaries. *Phys. Rev. B* **98**, 235147 (2018).
- [19] Nussinov, Z. & Ortiz, G. Sufficient symmetry conditions for Topological Quantum Order. *Proc. Nat. Acad. Sci.* **106**, 16944–16949 (2009).
- [20] Qiu, Y. & Wang, Z. Ground Subspaces of Topological Phases of Matter as Error Correcting Codes. *arXiv:2004.11982* (2020).
- [21] Terhal, B. M. Quantum error correction for quantum memories. *Rev. Mod. Phys.* **87**, 307–346 (2015).
- [22] Kitaev, A. Y. Fault-tolerant quantum computation by anyons. *Ann. Phys. (N. Y.)* **303**, 2–30 (2003).
- [23] Tagliacozzo, L. & Vidal, G. Entanglement renormalization and gauge symmetry. *Phys. Rev. B* **83**, 115127 (2011).
- [24] Trebst, S., Werner, P., Troyer, M., Shtengel, K. & Nayak, C. Breakdown of a Topological Phase: Quantum Phase Transition in a Loop Gas Model with Tension. *Phys. Rev. Lett.* **98**, 070602 (2007).
- [25] Wootton, J. A Simple Decoder for Topological Codes. *Entropy* **17**, 1946–1957 (2015).
- [26] Haah, J. Local stabilizer codes in three dimensions without string logical operators. *Phys. Rev. A* **83**, 042330 (2011).
- [27] Chamon, C. Quantum Glassiness in Strongly Correlated Clean Systems: An Example of Topological Overprotection. *Phys. Rev. Lett.* **94**, 040402 (2005).
- [28] Hastings, M. B. Topological Order at Nonzero Temperature. *Physical Review Letters* **107** (2011).
- [29] Bardyn, C.-E. *et al.* Topology by dissipation. *New J. Phys.* **15**, 085001 (2013).
- [30] Viyuela, O., Rivas, A. & Martin-Delgado, M. A. Two-Dimensional Density-Matrix Topological Fermionic Phases: Topological Uhlmann Numbers. *Phys. Rev. Lett.* **113**, 076408 (2014).
- [31] Huang, Z. & Arovas, D. P. Topological Indices for Open and Thermal Systems Via Uhlmann's Phase. *Phys. Rev. Lett.* **113**, 076407 (2014).
- [32] Grusdt, F. Topological order of mixed states in correlated quantum many-body systems. *Phys. Rev. B* **95**, 075106 (2017).
- [33] Roberts, S., Yoshida, B., Kubica, A. & Bartlett, S. D. Symmetry-protected topological order at nonzero temperature. *Phys. Rev. A* **96**, 022306 (2017).
- [34] Weimer, H., Müller, M., Lesanovsky, I., Zoller, P. & Büchler, H. P. A Rydberg quantum simulator. *Nature Phys.* **6**, 382–388 (2010).
- [35] Hinrichsen, H. Non-equilibrium critical phenomena and phase transitions into absorbing states. *Adv. Phys.* **49**, 815–958 (2000).

- [36] Ódor, G. Critical branching-annihilating random walk of two species. *Phys. Rev. E* **63**, 021113 (2001).
- [37] Kitaev, A. Y. Unpaired Majorana fermions in quantum wires. *Phys.-Usp.* **44**, 131 (2001).
- [38] Haldane, F. D. M. Nonlinear Field Theory of Large-Spin Heisenberg Antiferromagnets: Semiclassically Quantized Solitons of the One-Dimensional Easy-Axis Néel State. *Phys. Rev. Lett.* **50**, 1153–1156 (1983).
- [39] Brown, B. J. & Williamson, D. J. Parallelized quantum error correction with fracton topological codes. *Phys. Rev. Research* **2**, 013303 (2020).
- [40] Kitagawa, T., Berg, E., Rudner, M. & Demler, E. Topological characterization of periodically driven quantum systems. *Phys. Rev. B* **82**, 235114 (2010).
- [41] Lindner, N. H., Refael, G. & Galitski, V. Floquet topological insulator in semiconductor quantum wells. *Nature Phys.* **7**, 490–495 (2011).
- [42] Dennis, E., Kitaev, A., Landahl, A. & Preskill, J. Topological quantum memory. *J. Math. Phys.* **43**, 4452–4505 (2002).
- [43] Liu, F. *et al.* Circuit complexity across a topological phase transition. *Phys. Rev. Research* **2**, 013323 (2020).

I. SUPPLEMENTARY METHODS

A. From topological robustness to error correction

Let us describe how to perform a generalized construction of error correcting models for topologically ordered phases. We start by considering a topologically ordered phase having degenerate ground states $\{|g_\alpha\rangle\}$, where any quasilocal operator V satisfies

$$\langle g_\alpha | V | g_\beta \rangle = v \delta_{\alpha\beta} + c, \quad (\text{SM-1})$$

with c being either zero or vanishing in the thermodynamic limit [S1]. Here, the ground state index α defines a topological quantum number. We can take this topological quantum number to be the eigenvalue of an operator O_{topo} encoding topological order. For example, in the case of the toric code, O_{topo} is related to the non-trivial loop operators around the torus. We now separate the Hamiltonian H into a part containing the operator O_{topo} and a remaining part H_0 , i.e.,

$$H = H_0 + \lim_{h \rightarrow 0} h O_{\text{topo}}. \quad (\text{SM-2})$$

Since the topological quantum numbers describing a topological phase are good quantum numbers by construction, we have $[H, O_{\text{topo}}] = [H_0, O_{\text{topo}}] = 0$, at least in the thermodynamic limit. Importantly, H_0 has a unique ground state, as the topological ground state degeneracy of H is given by $\dim(O_{\text{topo}})$.

While it is tempting to try to analyze topological order by considering the operator O_{topo} [S2], its inherent nonlocality severely limits the possibility to make general statements about its properties. For example, arguments related to spontaneous symmetry breaking do not apply and hence do not allow to treat $\langle O_{\text{topo}} \rangle$ as a topological order parameter. Therefore, we completely neglect the operator O_{topo} in the following and entirely focus our discussion on the Hamiltonian H_0 .

As already mentioned, H_0 has a unique ground state $|\psi_0\rangle$, which is also invariant under all (possibly nonlocal) symmetry transformations of the original Hamiltonian H , as the topological degrees of freedom have been separated off in Eq. (SM-2). This means that $|\psi_0\rangle$ describes a quantum paramagnet (for spin systems) or an insulator (for bosons or fermions). Without loss of generality, we will use the terminology of spins systems in the following. Crucially, a paramagnet is adiabatically connected to the ground state $|\psi_p\rangle$ of the Hamiltonian

$$H_B = B \sum_{\mu} O_{\mu}, \quad (\text{SM-3})$$

with quasi-local commuting operators O_{μ} and B being a constant describing an effective magnetic field. The operators O_{μ} can be chosen such that their smallest eigenvalue is zero, meaning that the ground state satisfies $O_{\mu} \equiv 0$. Here, we use the index μ to indicate that the degrees of freedom of H_B are defined on a different lattice than the original model. Note that this does not imply that H_0 can be written in the form of Eq. (SM-3), as the fusion and braiding rules concerning *excited* states on top of $|\psi_p\rangle$ represent highly nontrivial interactions terms that are absent in Eq. (SM-3).

In the following, we choose the state $|\psi_r\rangle = |\psi_p\rangle|\alpha\rangle$ to serve as the reference state. Which value of α is chosen to define the reference state is actually not important as it will not affect any of the O_{μ} operators. Importantly, errors with respect to the reference state are described by violations of the constraint $O_{\mu} = 0$. Since the topological phase is protected by the gap of the paramagnet, the paramagnetic phase of H_0 is equivalent to the topologically ordered phase of H .

We note that classifying topological phases in terms of the reference state $|\psi_r\rangle$ is actually not that different from classifying conventional Landau symmetry breaking phases in terms of local order parameters, as each order parameter also defines a set of reference states that maximize the order parameter. Hence, all that is left to complete the operational definition of topological order in terms of its error correction abilities is to describe how to construct the syndrome operators O_{μ} from the reference state and how to perform the error correction.

Since the error syndrome operators O_{μ} are quasilocal, it is rather straightforward to identify them once the reference state is defined. In particular one can perform an operator expansion in terms of quasilocal operators \mathcal{O}_i (defined on the original lattice) to identify the lattice sites μ and the associated operators O_{μ} in the space of excitations on top of the reference state. For example, performing an operator expansion on top of the ground state of the toric code in terms of Pauli matrices gives rise to the well-known Ising map of the anyons [S3]. The set $\{O_{\mu}\}$ is the set of syndrome operators that needs to be measured before the error correction procedure can be carried out.

In the following, we assume that the syndrome operators O_{μ} have been measured M times, yielding a set of $O_{\mu}^{(r)}$ measurement results, where r running from 1 to M indicates the individual measurement run. The classification of

the phase then reduces to a purely classical problem: Which operations need to be applied, such that the reference state having $O_\mu \equiv 0$ is reached for a given configuration $O_\mu^{(r)}$ at fixed r ? Since the configurations differ for each value of r , this introduces a statistical element to the error correction circuit. However, since the problem is classical, the required error correction circuits can be computed for very large system sizes.

Let us now refer to the circuit depth n_d as a suitable statistical measure (e.g., the mean or the variance) over all M measurement results. The required operations can be constructed from the quasilocal operators \mathcal{O}_i used to define the syndrome operators, as applying their inverse will map the system back onto the reference state. Remarkably, these operations actually describe the fusion rules of the topological phase.

Denoting by d_H the Hamming distance (or higher-dimensional equivalent) to the reference state, i.e., the number of fusion processes needed to reach the reference state, we can introduce a simple error correction strategy. From each site μ containing an error, we perform a search of the surroundings of μ to find other nearby errors. Whenever we find a configuration that allows an operation that lowers d_H , it gets carried out. Although this error correction algorithm is not necessarily optimal, it is guaranteed to result in the desired reference state as d is decreasing monotonously. For the toric code, this strategy precisely yields the error correction algorithms described in the Methods section.

B. Many-body perturbation theory in the topological phase

Let us now turn to a scaling analysis of the circuit depth n_d of this error correction strategy. In the topologically ordered phase, we can define all the ground states in terms of a perturbative expansion on top of the Hamiltonian H_B and its ground state $|\psi_p\rangle$, respectively [S4]. Formally, the ground state of the perturbed Hamiltonian $H = H_B + \lambda V$ can be expressed as

$$|\psi\rangle = \frac{P}{\langle\psi_p|P|\psi_p\rangle}|\psi_p\rangle \quad (\text{SM-4})$$

using the projector $P = |\psi\rangle\langle\psi|$ given by

$$P = |\psi_p\rangle\langle\psi_p| + \sum_{k=0}^{\infty} \lambda^k A_{(k)} \quad (\text{SM-5})$$

Here, the operators $A_{(n)}$ have the form

$$A_{(k)} = \sum_{(k)} = -S_{l_1} V S_{l_2} V \cdots V S_{l_{k+1}}, \quad (\text{SM-6})$$

with the sum running over all sets of l_i satisfying $l_i \geq 0$ and $\sum_i l_i = k$. The resolvent operators S_l are given by

$$S_l = \begin{cases} |\psi_p\rangle\langle\psi_p| & \text{for } l = 0 \\ \sum_n \frac{|n\rangle\langle n|}{(E_0 - E_n)^l} & \text{for } l > 0 \end{cases}, \quad (\text{SM-7})$$

where $|n\rangle$ are the excited states of H_B with energies E_n . Importantly, the perturbation series is convergent as long as we stay in the topological phase, as there is no closing of the energy gap. Then, we can truncate the series at k_{max} th order, leaving an error in n_d that is exponentially small in k_{max} , i.e., $n_d < C n_{d,k_{max}}$, where C is a constant chosen to be independent of the system size N and $n_{d,k_{max}}$ is the circuit depth of the state truncated at order k_{max} . Since this expression does not involve the system size, it is clear that there exists a finite-depth error correction circuit. This finite-depth scaling is also reached by the error correction strategy described above, as it is bounded by the largest cluster size encountered in the perturbative expansion, which again is a function of k_{max} and not of the system size.

C. Maximally random errors in the trivial phase

Importantly, the perturbative argument discussed above breaks down once the system is outside the topological phase, e.g., in a trivial phase, as the perturbation series diverges in this case. To establish the circuit depth scaling for trivial states, let us turn to the error correction properties of topological phases. We consider a topologically trivial product state of all spins pointing in the x direction. Such a state has no bit-flip errors (or higher dimensional equivalents), meaning the O_μ^{bit} describing such errors are still zero. On the other hand, the O_μ^{phase} related to phase flip

errors are maximally random. This maximum randomness is reached if all configurations of the phase error syndrome $\{O_\mu^{\text{phase}}\}$ are equally likely.

In the following, we consider the mean circuit depth, i.e.,

$$\bar{n}_d = \frac{1}{M} \sum_r n_d^{(r)}, \quad (\text{SM-8})$$

where $n_d^{(r)}$ refers to the circuit depth for a given set of measurements $O_\mu^{(r)}$. We then proceed by noting that $n_d^{(r)}$ can be bounded from below by considering a 2D torus topology containing a single error type (encoding the aforementioned phase errors) that can be removed by an m -ary fusion process, as adding more error types, higher dimensionality, or open boundaries will always increase $n_d^{(r)}$. However, treating different m separately is necessary as we will see below that there is no choice of m that leads to a minimal $n_d^{(r)}$ for all error configurations. For $m = 2$, this simplification yields the toric code model in the limit of an infinite magnetic field.

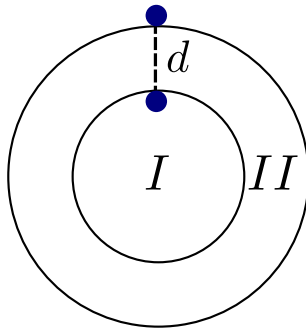


FIG. SM-1. Removal of the last errors. Two parts of the system I and II , each containing N/p sites are introduced. With finite probability, the last error in the part I has to be fused across an empty region II , requiring at least d steps for the error correction to complete.

Now, let us show that for the trivial state introduced above, the circuit depth diverges in the thermodynamic limit. To achieve this, we look at two neighboring parts within the bulk of the system, one being a circle and the other a ring surrounding the first part, see Fig. SM-1. Each part contains N/p sites, where p is a constant independent of the system size N . To simplify the analysis, we neglect all error correction steps that occur before we arrive at less than m errors in the two patches. Obviously, the remaining steps $n_p^{(r)}$ set again a lower bound on $n_d^{(r)}$. Since all error configurations are equally likely in the topologically trivial state under consideration, the remaining number of errors N_ε is uniformly distributed between 0 and $m - 1$. Let us now specialize on the case $N_\varepsilon = 1$, which occurs with a probability of $1/m$. Again, the one remaining error can be located in either of the two patches with a probability of $1/2$. In the case where this single error is located in the outer ring, one might get lucky and find the remaining $m - 1$ fusion partners just outside the ring and the remaining circuit depth is small. However, when the final error is located in the center patch, finding the fusion partners will require at least

$$d = (\sqrt{2} - 1) \sqrt{\frac{N}{\pi p}} \quad (\text{SM-9})$$

steps as the width d of the empty ring has to be crossed. Since this configuration occurs with a probability of $1/2m$, the overall circuit depth has to satisfy

$$n_d \geq \frac{\sqrt{2} - 1}{2m} \sqrt{\frac{N}{\pi p}} \quad (\text{SM-10})$$

which diverges in the thermodynamic limit.

Consequently, the circuit depth n_d is always finite in the topologically ordered phase, while it diverges in the trivial phase. This demonstrates that the circuit depth can be successfully used in the classification of topologically ordered phases of matter.

II. SUPPLEMENTARY DISCUSSION

A. Error correction for the cubic code

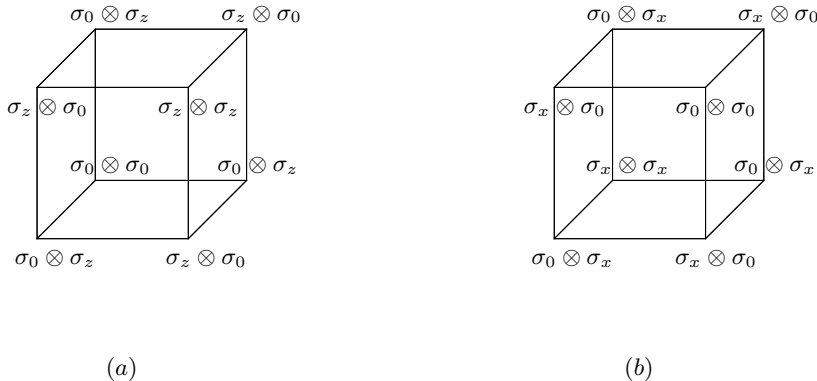


FIG. SM-2. Sketch of the cubic code model. Decomposition of the operators A_c (a) and B_c (b) in terms of Pauli matrices σ_x and σ_z , with σ_0 being the identity.

The cubic code [S5] is a paradigmatic model for fracton excitations, i.e., the fusion of the errors is no longer described by a linear string operator as in the toric code, but an operator that involves the sites inside the volume spanned by the errors in a fractal shape. The Hamiltonian of the cubic code has the same structure as the toric code, i.e.,

$$H = -E_0 \sum_c (A_c + B_c). \quad (\text{SM-11})$$

The crucial properties of the cubic code arise from the definition of the A_c and B_c operators. As shown in Fig. SM-2, both operators are defined in terms of the cubes c , with each vertex of the cube supporting two spin-1/2 lattice sites. Owing to the arrangement of the Pauli matrices σ_x and σ_z , flipping a single spin will result in the appearance of four errors arranged in a tetrahedron, see Fig. SM-3. These errors can no longer be moved around by additional flips of single spins, as such an operation would remove one error and create three additional ones, i.e., changing the number of errors and thus the energy of the system. Instead, moving errors require the application of an operator that involves the spins inside the tetrahedron in a fractal shape.

Nevertheless, error correction in the cubic code can be implemented in the usual way, with the reference state being one of the ground states of Eq. (SM-11). Here, each walker has to search for the existence of two other errors located at the vertices of a tetrahedron. If such triples of errors can be found, fusion using the fractal operator will lower the Hamming distance to the reference state, even if the fourth vertex of the tetrahedron does not contain an error.

Having specified the error correction algorithm, we can also look into the consequences for the circuit depth. In the fracton phase, the perturbative argument introduced in Sec. IA holds and the circuit depth is finite. For the trivial phase, we consider the case where all error syndromes for one error type (e.g., A_c) are equally likely. In this case, there are again configurations occurring with finite probability that require the application of a thermodynamically large fractal operator (i.e., diverging with N). From this, we conclude that we can also successfully classify fracton phases using our error correction approach.

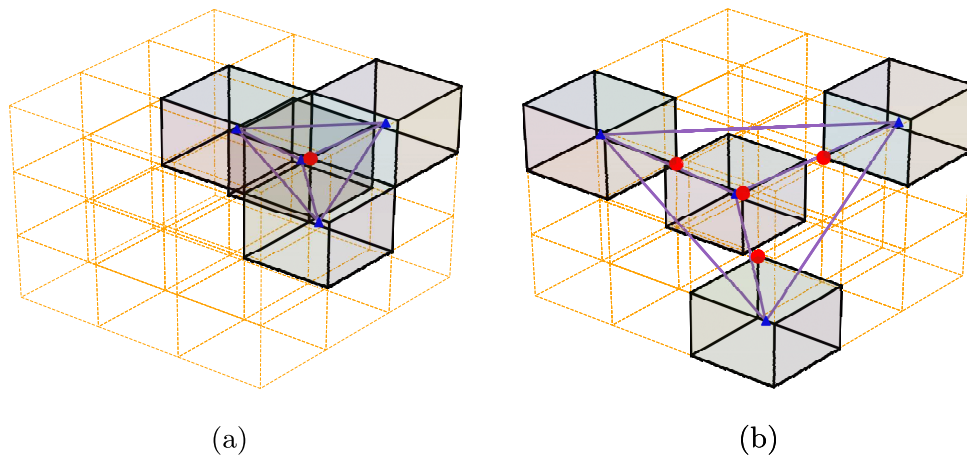


FIG. SM-3. Errors of the cubic code. (a) Applying a single spin-flip operator (red) to the ground state creates four errors (blue) shaped in a tetrahedron form. (b) The errors can be moved around by increasing the size of the tetrahedron by applying three additional spin-flip operators.

-
- [S1] Z. Nussinov and G. Ortiz, Sufficient symmetry conditions for Topological Quantum Order, *Proc. Nat. Acad. Sci.* **106**, 16944 (2009).
- [S2] M. den Nijs and K. Rommelse, Preroughening transitions in crystal surfaces and valence-bond phases in quantum spin chains, *Phys. Rev. B* **40**, 4709 (1989).
- [S3] S. Trebst, P. Werner, M. Troyer, K. Shtengel, and C. Nayak, Breakdown of a Topological Phase: Quantum Phase Transition in a Loop Gas Model with Tension, *Phys. Rev. Lett.* **98**, 070602 (2007).
- [S4] A. Messiah, *Quantum Mechanics, Vol. II* (North-Holland, Amsterdam, 1961).
- [S5] J. Haah, Local stabilizer codes in three dimensions without string logical operators, *Phys. Rev. A* **83**, 042330 (2011).